

Chiral Dynamics of Low-Energy Kaon-Baryon Interactions with Explicit Resonance

B. Krippa** and J.T.Londergan

*Department of Physics and Nuclear Theory Center, Indiana University,
2401 Milo Sampson Lane, Bloomington, IN 47408.*

Abstract

The processes involving low energy $\bar{K}N$ and $Y\pi$ interactions (where $Y = \Sigma$ or Λ) are studied in the framework of heavy baryon chiral perturbation theory with the $\Lambda(1405)$ resonance appearing as an independent field. The leading and next-to-leading terms in the chiral expansion are taken into account. We show that an approach which explicitly includes the $\Lambda(1405)$ resonance as an elementary quantum field gives reasonable descriptions of both the threshold branching ratios and the energy dependence of total cross sections.

PACS Nos: (13.75.Gx; 12.38.Lg; 11.55.Hx; 14.20.Dh)

***On leave from the Institute for Nuclear Research of the Russian Academy of Sciences, Moscow, 117312, Russia.*

I. INTRODUCTION

Heavy Baryon Chiral Perturbation Theory (HB χ PT) applied to the scattering amplitudes for processes involving baryons and mesons has been successful in describing experimental data for a significant number of low-energy meson-baryon interactions [1]. This method involves expansion in powers of the momentum for sufficiently low energies. As the number of terms in such expansions grows exponentially with energy, processes reasonably close to threshold are generally well described by this method. However, chiral expansions based on HB χ PT encounter a serious problem when they are used in systems with a resonance or bound state at threshold. As such systems possess an S-matrix pole, the standard low-order expansion techniques of chiral perturbation theory cannot provide a satisfactory description. Near a resonance the particles can in principle interact an infinite number of times, producing a characteristic energy dependence which cannot be reproduced by a power series with a small number of terms.

One system in which such a state appears is the NN system in the singlet channel, which is strongly affected near threshold by the “singlet deuteron” state. The problem of formulating a consistent chiral expansion for this channel has recently attracted much attention [2–6]. Low-energy K^-p interactions are also, to a large extent, governed by the subthreshold $\Lambda(1405)$ resonance. In the present paper we focus on the $\overline{K}N$ and $Y\pi$ systems (where Y includes the Λ and Σ hyperons) at low energy.

Two methods have been suggested so far to formulate a chiral approach to reactions in the presence of a low-energy or subthreshold resonance. In the first method [7], one uses just the tree level irreducible diagrams, generated by HB χ PT in leading and subleading order, to construct an effective potential. This potential is then inserted into the Lippmann-Schwinger equation, which iterates the effective potential to all orders. A sufficiently attractive effective potential will generate a resonance when iterated in this manner. Using this method Kaiser, Siegel and Weise [7] were able to generate the $\Lambda(1405)$ resonance dynamically, and obtained good fits to experimental data in this nonperturbative scheme.

Although iteration of an effective potential allows one to reproduce low-energy interactions in the vicinity of a resonance pole, this represents a substantial departure from HB χ PT methods. In the standard HB χ PT analysis, all possible amplitudes are evaluated to a given order in the chiral expansion, whereas only ladder diagrams were summed up using the Lippmann-Schwinger equation. Second, in chiral expansions one can in principle remove the dependence of low energy constants on the regularization parameter by using the renormalization group equations. Using the Lippmann-Schwinger equation, it is necessary to impose a cutoff in order to render the integral part of the Lippmann-Schwinger equation finite. Moreover, it turns out that the results of calculations depend rather strongly on the value of the cutoff [8]. Third, as is well known in scattering theory, effective potentials which give identical on-shell results can in principle differ in their off-shell extrapolation, so that the results of the Lippmann-Schwinger calculations will also depend on the functional form used for the effective potential.

In the second approach, proposed by Lee, Min and Rho [9], the $\Lambda(1405)$ resonance is treated from the beginning as an "elementary" field which participates on an equal footing with all other quantum fields in the chiral Lagrangian. It was shown in Ref. [9] that in the framework of such an approach one can obtain reasonable threshold branching ratios for $\overline{K}N$ and $Y\pi$ channels, taking into account only the leading order $\mathcal{O}(Q)$ terms. However, in Ref. [9] only the lowest order chiral Lagrangian was used in the actual calculations, and the authors did not compare their model with experimental data for reaction channels involving an initial-state K^-p system. In the present paper we explore the approach suggested in Ref. [9], in which the $\Lambda(1405)$ is included in the Lagrangian as an elementary field. We take their calculation one step further by including the next-to-leading order terms in the chiral Lagrangian, and we compare our results to experimental reaction cross sections near threshold.

II. EFFECTIVE CHIRAL LAGRANGIAN

The effective chiral Lagrangian can be written as a sum of terms each of which is proportional to a particular power of the characteristic momentum which we denote Q . Then the physical amplitude can be represented as a power series in Q . The chiral counting rules can be used to determine the chiral dimension of the amplitude at any given order. The leading order terms are linear in Q , while the next-to-leading terms go as Q^2 . To this order the Lagrangian we are interested in is given by [7]

$$\mathcal{L} = \mathcal{L}^{(1)} + \mathcal{L}^{(2)} \quad (1)$$

where the leading order term is given by

$$\mathcal{L}^{(1)} = \frac{i}{8f^2} \text{Tr}(\bar{B}[\phi, \partial_0 \phi], B) + (\sqrt{2}g_{\Lambda^*} \bar{\Lambda}^* \text{Tr}((v \cdot A)B) + h.c.) \quad (2)$$

and the next-to-leading order term of the effective Lagrangian can be written as follows

$$\begin{aligned} \mathcal{L}^{(2)} = & \frac{i}{2M_0} \text{Tr}(\bar{B}((v \cdot D)^2 - D^2)B) + b_D \text{Tr}(\bar{B}\{\chi_+, B\}) + b_F \text{Tr}(\bar{B}[\chi_+, B]) + b_0 \text{Tr}(\bar{B}B) \text{Tr}(\chi_+) \\ & + d_D \text{Tr}(\bar{B}\{A^2 + (v \cdot A)^2, B\}) + d_F \text{Tr}(\bar{B}[A^2 + (v \cdot A)^2, B]) + d_0 \text{Tr}(\bar{B}B) \text{Tr}(A^2 + (v \cdot A)^2) \\ & + d_1 \left[\text{Tr}(\bar{B}A_\nu) \text{Tr}(A^\nu B) + \text{Tr}(\bar{B}(v \cdot A)) \text{Tr}((v \cdot A)B) \right] + \\ & d_2 \text{Tr} \left[\bar{B}(A_\nu B A^\nu + (v \cdot A)B(v \cdot A)) \right] \end{aligned} \quad (3)$$

We define the chiral covariant derivative $D^\nu B = \partial^\nu B + [\Gamma^\nu, B]$ with a chiral connection Γ^ν and axial operator $A_\nu = -\frac{1}{2f} \partial_\nu \phi$ where B and ϕ are baryon and meson field matrices in standard form [7]. The matrix χ_+ is given by

$$\chi_+ = -\frac{1}{4f^2} \{\phi, \{\phi, \chi\}\} \quad (4)$$

where χ is the meson mass matrix with the diagonal elements $(m_\pi^2, m_\pi^2, 2m_K^2 - m_\pi^2)$. The field Λ^* describes the state $\Lambda(1405)$ introduced as an elementary field with Λ^*KN coupling constant $g_{\Lambda^*}^2=0.15$. As in Ref. [9] this value was extracted from the decay width $\Gamma=50$ MeV for the process $\Lambda(1405) \rightarrow \pi\Sigma$. The first term in the Lagrangian $\mathcal{L}^{(2)}$ describes the $1/M$

corrections. The form of this term follows directly from the corresponding relativistic expression and does not contain the unknown low-energy constants. The low-energy constants in front of the terms with the double derivatives and mass terms are not determined by chiral symmetry and must therefore be extracted from the experimental data. The procedure we used to determine the constants $\{b\}$ in Eq. 3 is similar to that used in Ref. [7]. The constants b_D and b_F can be extracted from the baryon mass splittings. Using the $SU(3)$ relations for the baryon masses one can get the values $b_D = 0.06 \text{ GeV}^{-1}$ and $b_F = -0.22 \text{ GeV}^{-1}$. The constant b_0 can be related to the πN sigma term. To the order we are interested in, this relation is given by

$$\sigma_{\pi N} = -2m_\pi^2(b_D + b_F + 2b_0) \quad (5)$$

In our calculations we used the value $b_0 = -0.34 \text{ GeV}^{-1}$. The uncertainty in the value of b_0 arises mainly from the uncertainty in the pion-nucleon sigma term

The unknown effective constants $\{d\}$ associated with the terms with double derivatives in Eq. 3 can be extracted from experimental data. There are six channels ($\pi\Sigma, \pi\Lambda, \bar{K}N$) which can be involved in the dynamics of K^-p interactions at low energies. There are also relations for the isospin-even πN S-wave scattering length $a_{\pi N}^+$ and isospin zero kaon-nucleon S-wave scattering length a_{KN}^0 , which are given by the following expressions

$$4\pi(1 + \frac{m_\pi}{M_N})a_{\pi N}^+ = \frac{m_\pi^2}{f^2}(d_D + d_F + 2d_0 - 2b_D - 2b_F - 4b_0 - \frac{g_A^2}{4M_N}) \quad (6)$$

and

$$4\pi(1 + \frac{m_K}{M_N})a_{KN}^0 = \frac{m_K^2}{f^2}(-2d_F + 2d_0 - d_1 + 4b_F - 4b_0 - \frac{D}{M_N}(F - D/3)) \quad (7)$$

Here g_A is the axial vector coupling constant and F and D are the $SU(3)$ coupling constants which satisfy the relation $D + F = 1.26$. Eq. 7 puts constraints on the possible values of the effective constants $\{d\}$. We have used the experimental data from Refs [10] and [11]. Both scattering lengths are very small: $a_{\pi N}^+ = (-0.012 \pm 0.06) \text{ fm}$ and $a_{KN}^0 = (-0.1 \pm 0.1) \text{ fm}$. One notes that in the expression for $a_{\pi N}^+$ we have not included the term corresponding

to the non-analytic loop correction proportional to m_π . Since we calculate the scattering amplitudes up to order Q^2 it would not be consistent to include at any point terms stemming from loop corrections which are of order Q^3 . After imposing the constraints we are left with three undetermined constants. We fix the remaining constants using the experimental data describing the energy dependence of the total cross sections of the reaction channels with a K^-p system in the initial state. There are six possible final channels altogether, so after fixing three constant we obtain theoretical predictions for three reaction channels.

III. RESULTS AND DISCUSSION

First, we fix the low-energy constants $\{d\}$ which appear in Eq. 3. We work in the limit of conserved isospin and use the the following masses: $m_\pi=139.6$ MeV, $m_K=493.6$ MeV, $M_N=938.3$ MeV, $M_\Lambda=1115.6$ MeV, and $M_\Sigma=1192.5$ MeV. A set of low-energy constants $\{d\}$ which give a reasonable description of the experimental data are given in Table I. We compare these constants with the same quantities defined by Kaiser *et al.* [7]. These authors expand the chiral Lagrangian to second order without an elementary $\Lambda(1405)$ field. The resonance is obtained by using the low-order chiral expansion as a potential, and generating the resonance by iterating the potential in the Lippmann-Schwinger equation. Although the sign of each term is the same, the absolute values of the effective constants differ considerably from those obtained in Ref. [7]. Thus, although the results of the two approaches are in good quantitative agreement (e.g., the very similar values for the reaction cross sections given in Figs. 1-6 of this paper, and those of Kaiser *et al.*, Ref. [7]), the coefficients of the corresponding “expansion constants” in the Lagrangian are very different. The differences between expansion parameters are not surprising, given the different Ansatz regarding the origin of the $\Lambda(1405)$ resonance. If one treats the low-order chiral expansion as a potential and iterates it in ladder approximation to obtain the $\Lambda(1405)$, then the expansion constants of Ref. [7] are appropriate. If one treats the $\Lambda(1405)$ as an elementary field coupled to the $\bar{K}N$ system, then the expansion constants of the “residual” system are given by our values.

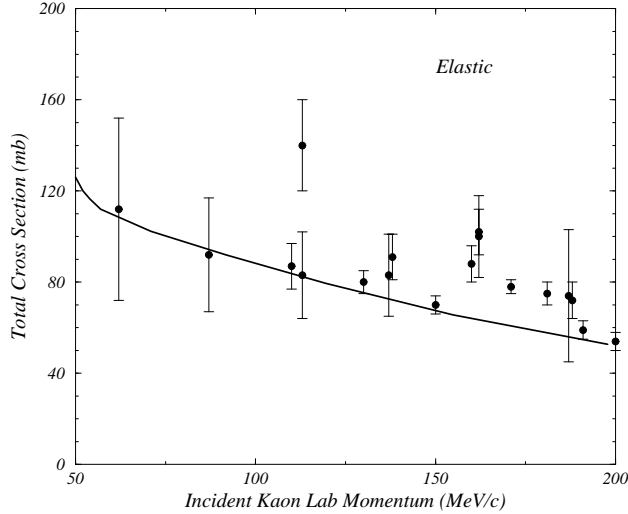


FIG. 1. Results of our theoretical calculations compared with experimental data [12,13] for K^-p elastic scattering.

In Figs. 1-6, we compare the results of our calculations of the total cross sections for all channels with the experimental data [12,13]. The agreement with experiment is quite reasonable, indicating that the leading and subleading contributions including an explicit $\Lambda(1405)$ resonance play a dominant role in the low-energy dynamics of the K^-p system. It is worth mentioning that without the contribution from the $\Lambda(1405)$ resonance the probability for the process $K^-p \rightarrow \pi^-\Sigma^+$ would be suppressed at leading order. Moreover, the cross sections of other reactions would also be much too low. The one case where our calculations fails to reproduce experiment is the $K^-p \rightarrow \pi^0\Lambda$ channel shown in Fig. 5, where our calculated cross section is lower than the experimental data. This is probably due to the fact that the $\Lambda(1405)$ resonance, which is a prominent feature for all other channels, does not contribute to this transition. To bring this cross section closer to the experimental value will probably require calculating the loop corrections for the reaction $K^-p \rightarrow \pi^0\Lambda$. So, for all reaction channels where the $\Lambda(1405)$ resonance contributes, it is an important ingredient in producing a realistic description of the experimental data.

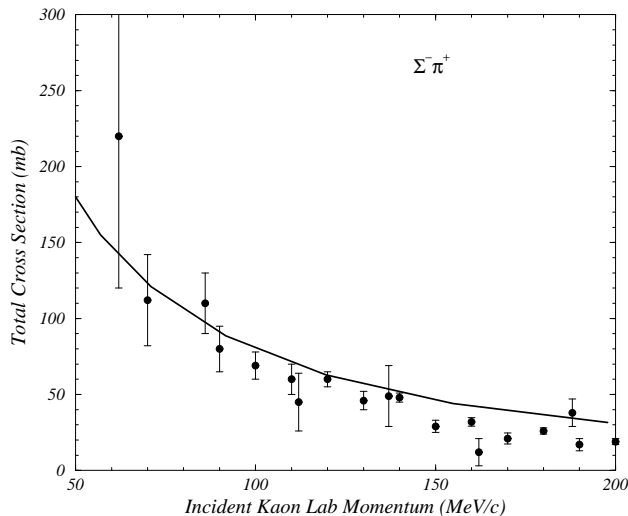


FIG. 2. Results of our theoretical calculations compared with experimental data [12,13] for the reaction $K^-p \rightarrow \Sigma^- \pi^+$.

Our predicted cross sections agree favorably with those calculated by Kaiser *et al.*, Ref. [7]. They used the next-to-leading order contribution (not including an explicit $\Lambda(1405)$ field) as an effective potential, and iterated this to all orders in a Lippmann-Schwinger equation. By introducing an explicit $\Lambda(1405)$ “elementary” field, we are able to obtain qualitatively similar results to Kaiser *et al.*, except for the channel $K^-p \rightarrow \Lambda \pi^0$ as discussed previously.

The other major difference between the two calculations is that the iterated potential results are able to obtain cusps at inelastic thresholds, where we do not obtain cusp behavior. Since we are neglecting $\mathcal{O}(Q^3)$ corrections, we do not expect our calculations to be able to reproduce subtle features like threshold cusps. Such cusps appear in theoretical calculations as the energy of the incoming kaon crosses the threshold energy of a reaction channel. Threshold cusps have not been seen in the experimental data for K^-p reactions. However, the data are characterized by rather large error bars so that cusp singularities could very well be hidden within the present experimental uncertainties. Such cusps have proven notoriously difficult to observe in reaction cross sections.

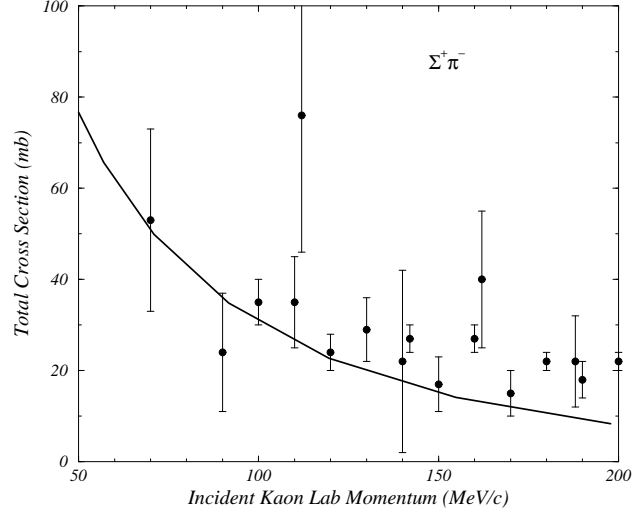


FIG. 3. Results of our theoretical calculations compared with experimental data [12,13] for the reaction $K^-p \rightarrow \Sigma^+\pi^-$.

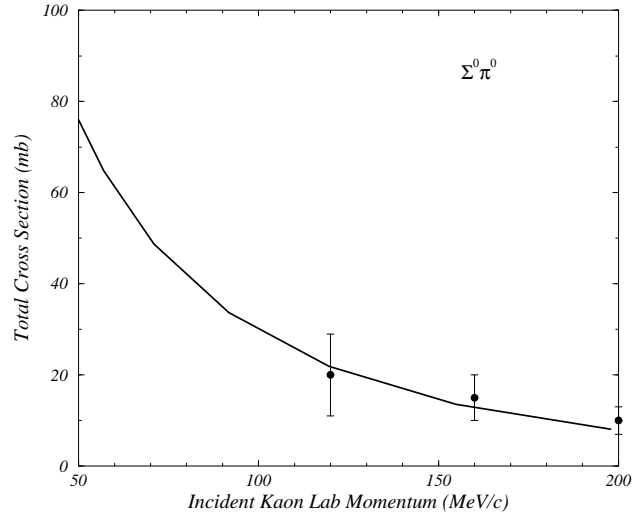


FIG. 4. Results of our theoretical calculations compared with experimental data [12,13] for the reaction $K^-p \rightarrow \Sigma^0\pi^0$.

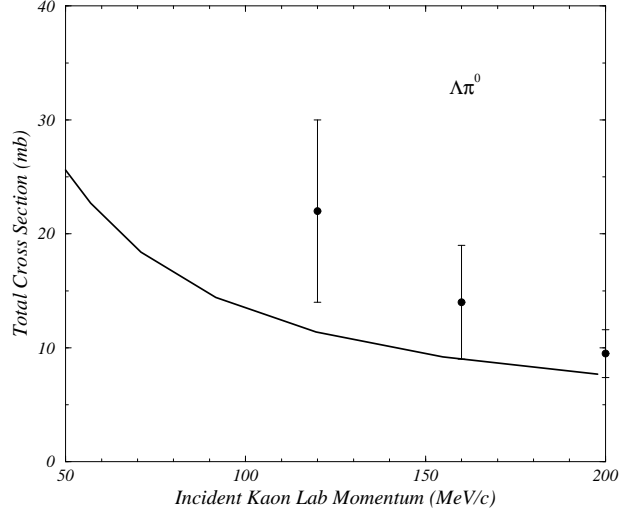


FIG. 5. Results of our theoretical calculations compared with experimental data [12,13] for the reaction $K^-p \rightarrow \Lambda\pi^0$.

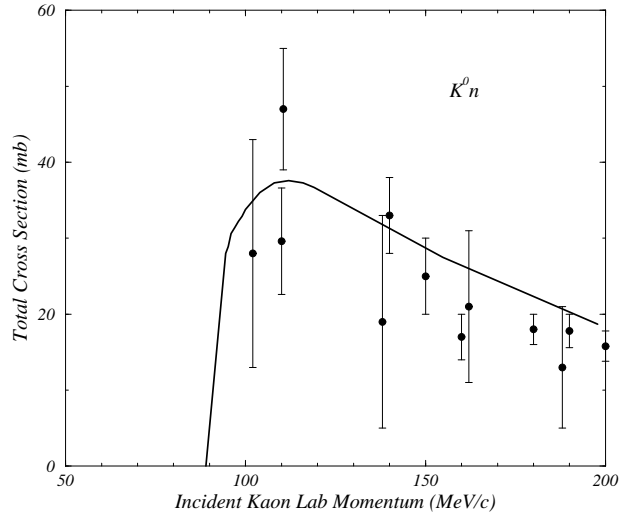


FIG. 6. Results of our theoretical calculations compared with experimental data [12,13] for the reaction $K^-p \rightarrow K^0n$.

Next we make a few remarks concerning the loop corrections. They start to contribute at order $\mathcal{O}(Q^3)$ and are necessary to ensure unitarity and take into account the effect of coupled channels. In addition, the $1/M^2$ and $SU(3)$ violating effects should also be included at this order. However, all one loop corrections in an $SU(3)$ multiplet need to be taken into account in a consistent formalism. At present, such a program would not be feasible since at this order the number of low-energy constants (needed to absorb divergences of the loop diagrams) would be much larger than the number of observables available to fix these constants.

In our calculation we keep the mass of the $\Lambda(1405)$ resonance real, *i.e.* we treat it as a zero-width resonance. It would not be consistent to include the width of the $\Lambda(1405)$ state since the width arises from loop corrections, and thus is of higher order. We also keep the coupling constant g_{Λ^*} the same for all channels involved. This is an exact result in the limit of perfect $SU(3)$ symmetry. The coupling constants in various channels may differ when we include terms of order $\mathcal{O}(Q^3)$. The leading $SU(3)$ violating corrections to the coupling constant g_{Λ^*} have been computed in Ref. [14]. These corrections reduce the value of the $\overline{K}N$ coupling compared to $\Sigma\pi$. To evaluate how these corrections affect the results of calculations, one needs to include all possible one loop corrections. As we noted previously, that is not feasible at present due to the large number of unconstrained constants.

The other interesting physical quantities in low-energy K^-p scattering are the threshold branching ratios

$$\begin{aligned}\gamma &= \frac{\Gamma(K^-p \rightarrow \pi^+\Sigma^-)}{\Gamma(K^-p \rightarrow \pi^-\Sigma^+)} = 2.36 \pm 0.04 \\ R_c &= \frac{\Gamma(K^-p \rightarrow \text{charged particles})}{\Gamma(K^-p \rightarrow \text{all})} = 0.664 \pm 0.011 \\ R_n &= \frac{\Gamma(K^-p \rightarrow \pi^0\Lambda)}{\Gamma(K^-p \rightarrow \text{all neutral states})} = 0.189 \pm 0.015\end{aligned}\tag{8}$$

The experimental values are taken from Refs. [12] and [13]. In Table II we show the theoretical results for the branching ratios of Eq. 8, compared with the experimental values. The leading order results, of order $\mathcal{O}(Q^1)$, were calculated earlier by Lee *et al.*, Ref. [9].

They can be compared with our results calculated to order $\mathcal{O}(Q^2)$. Taking into account the next-to-leading corrections in the effective chiral Lagrangian clearly leads to significant improvement in the theoretical description. The second order contributions to γ and R_c constitute 18% and 48% corrections, respectively, to the first-order results, and make the resulting branching ratios in very good agreement with experiment. Although the branching ratio R_n is significantly increased over the lowest-order result, it is still much lower than the experimental result. The discrepancy probably arises for the same reason that we fail to fit the $K^-p \rightarrow \pi^0\Lambda$ cross section, namely that the $\Lambda(1405)$ resonance does not contribute to this reaction, and that higher-order loop corrections will presumably be necessary to reproduce this branching ratio. More precise measurements of all of these reactions would be very useful in constraining the parameters of the chiral Lagrangians.

IV. CONCLUSIONS

We have applied the effective chiral Lagrangian to describe low-energy interactions in channels coupled to the K^-p system. Our Lagrangian includes the terms of leading and next-to-leading order supplemented by a term describing the process of formation and decay of the $\Lambda(1405)$ resonance. In our approach the $\Lambda(1405)$ state appears as an independent quantum field, on the same footing as any other meson or baryon field included in the chiral Lagrangian. The effective low-energy constants were extracted from the available experimental data on the different reactions involving a K^-p channel in the initial state. Constraints on the expansion parameters were provided by fitting the isospin-even πN S-wave scattering length $a_{\pi N}^+$ and isospin zero kaon-nucleon S-wave scattering length a_{KN}^0 . The $\Lambda(1405)$ provides a dominant effect in practically every reaction channel, with the exception of the $K^-p \rightarrow \Lambda\pi^0$ process.

We obtained satisfactory agreement between our theoretical calculations and the experimental cross sections. We also analyzed three threshold branching ratios. In two cases we obtained very good agreement with the data, and inclusion of the second-order contribution

significantly improved the calculated branching ratio. For the branching ratio R_n , although the second-order result was twice as large as the branching ratio obtained in leading order, the theoretical result remained far below experiment. The loop corrections, which are needed to take into account unitarity and coupled channel effects, might help to correct the theoretical prediction for the ratio R_n . Such calculations, however, are not feasible at present because one has more effective constants (needed to absorb divergences appearing in the loop integrals) than can be fixed from experimental data.

A natural extension of our formalism would be to analyze the processes of photo- and electroproduction of a kaon from a proton. This extension is clearly parameter free. Experimental data exist for the reactions $\gamma p \rightarrow K^+ \Lambda$ and $\gamma p \rightarrow K^+ \Sigma$ [15]. An analysis of these experimental data would help constrain the known low energy effective constants, and would determine the values of previously unknown constants. Extending the calculations to such reactions might provide enough constraints that we could include loop corrections, which are necessary to make this approach fully consistent.

ACKNOWLEDGMENTS

One of us (B.K) would like to thank Prof. B.Holstein for stimulating discussions, and the Indiana University Nuclear Theory Center for the warm hospitality extended to him during his visit. This work was supported in part by the National Science Foundation under contract NSF-PHY-9722706.

REFERENCES

- [1] For some recent reviews see: G.Ecker, Proc. of International Workshop on Hadron Physics 96: Topics on the Structure and Interactions of Hadronic Systems, ed. E. Ferreira, V.L. Baltar and T de sa Borges (World Scientific, 1997), p. 125; Ulf-G. Meißner, Proceedings of Second International Symposium on Meson-Nucleon Physics and the Structure of the Nucleon, Vancouver BC, Aug. 1997, to be published (preprint **hep-ph/9707461**).
- [2] S.Weinberg, Phys. Lett. **B251**, 288 (1990); Nucl. Phys. **B363**, 3 (1991).
- [3] S.R.Beane, T.D.Cohen and D.R.Phillips, Nucl. Phys. **A631**, 447c (1998); preprint (**nucl-th/9709062**), unpublished.
- [4] G.P.Lepage, Lectures at the VIII Jorge Andre Swieca Summer School, Brazil 1997, to be published (preprint **nucl-th/9706029**).
- [5] D.B. Kaplan, Martin J. Savage and Mark B. Wise, to be published (preprint **nucl-th/9801034**).
- [6] K.G.Richardson, M.C.Birse and J.A.McGovern, to be published (preprint **hep-ph/9708435**).
- [7] N.Kaiser, P.B.Siegel and W.Weise, Nucl. Phys. **A594**, 325 (1995)
- [8] B.V.Krippa, Phys. Rev. **C**, to be published (preprint **hep-ph/9803332**).
- [9] C.-H.Lee, D.-P.Min and M.Rho, Nucl. Phys. **A602**, 334 (1996).
- [10] R.Koch, Nucl. Phys. **A448**, 707 (1986).
- [11] C.Dover and G.Walker, Phys. Rep. **89**, 1 (1982).
- [12] R.J. Nowak *et al.*, Nucl. Phys. **B139**, 61 (1978).
- [13] D.N. Tovee *et al.*, Nucl. Phys. **B33**, 493 (1971).

- [14] M.Savage, Phys. Lett. **B331**, 411 (1994).
- [15] M.Bockhorst *et al.*, Z. Phys. **C63**, 37 (1994)

FIGURE CAPTIONS

- FIG.1 Results of our theoretical calculations compared with experimental data [12,13] for K^-p elastic scattering.
- FIG.2 Results of our theoretical calculations compared with experimental data [12,13] for the reaction $K^-p \rightarrow \Sigma^- \pi^+$.
- FIG.3 Results of our theoretical calculations compared with experimental data [12,13] for the reaction $K^-p \rightarrow \Sigma^+ \pi^-$.
- FIG.4 Results of our theoretical calculations compared with experimental data [12,13] for the reaction $K^-p \rightarrow \Sigma^0 \pi^0$.
- FIG.5 Results of our theoretical calculations compared with experimental data [12,13] for the reaction $K^-p \rightarrow \Lambda \pi^0$.
- FIG.6 Results of our theoretical calculations compared with experimental data [12,13] for the reaction $K^-p \rightarrow K^0 n$.

TABLE I. Low-energy expansion constants for the chiral Lagrangian of Eq. 3. Our constants are compared with the local and separable chiral potentials of Kaiser *et al.*, Ref. [7].

Model	d_D	d_F	d_0	d_1	d_2
Kaiser local	-0.02	-0.29	-0.66	0.23	-0.39
Kaiser sep'l	-0.24	-0.43	-0.40	0.28	-0.62
Our values	-1.70	-0.10	-0.45	0.02	-2.3

TABLE II. Threshold branching ratios in chiral perturbation expansion with elementary $\Lambda(1405)$ field. Branching ratios are defined in Eq. 8. Our second-order branching ratios are compared with those obtained from the lowest-order calculation of Ref. [9].

Ratio	$\mathcal{O}(Q^1)$	$\mathcal{O}(Q^2)$	Expt.
γ	1.93	2.27	2.36 ± 0.04
R_c	0.46	0.679	0.664 ± 0.011
R_n	0.025	0.051	0.189 ± 0.015